Alexandria Engineering Journal (2016) 55, 2367–2373

HOSTED BY

ELSEVIER

Alexandria University

Alexandria Engineering Journal

www.elsevier.com/locate/aej
www.sciencedirect.com

ORIGINAL ARTICLE

Numerical investigation of magnetohydrodynamic stagnation point flow with variable properties

Muhammad Ijaz Khan [a,*], M.Z. Kiyani [a], M.Y. Malik [a], T. Yasmeen [b,c], M. Waleed Ahmed Khan [a], T. Abbas [a]

[a] *Department of Mathematics, Quaid-I-Azam University, 45320, Islamabad 44000, Pakistan*
[b] *Department of Mechanical Engineering, Imperial College London, London SW7 2AZ, UK*
[c] *Department of Mechanical Engineering, University of Engineering & Technology Peshawar, Pakistan*

Received 19 March 2016; revised 19 April 2016; accepted 28 April 2016
Available online 27 May 2016

KEYWORDS

Magnetohydrodynamics (MHDs);
Powell–Eyring fluid;
Stretching cylinder;
Stagnation point flow;
Variable thermal conductivity

Abstract This article is concerned with the two-dimensional flow of Powell–Eyring fluid with variable thermal conductivity. The flow is caused due to a stretching cylinder. Temperature dependent thermal conductivity is considered. Both numerical and analytic solutions are obtained and compared. Analytic solution is found by homotopy analysis method. Numerical solution by shooting technique is presented. Discussion to different physical parameters for the velocity and temperature is assigned. It is observed that the velocity profile enhances for larger magnetic parameter. It is also further noted that for increasing the value of Prandtl number temperature profile decreases.

1. Introduction

The researchers at present have much interest in the investigation of non-Newtonian liquids. It is due to their exceedingly significance in numerous organic, mechanical and designing procedures, for example, glass arrangement, fiber sheet fabricating, wire drawing, sustenance items, paper creation, precious stone development and so on. Analysis of boundary layer flow has special significance in the situations when fluid is passing over the surface. The researchers in recent times are looking for increasing the efficiency of various machines through reduction of drag/friction forces. Different endeavors therefore have been made about lessening of drag powers/forces for flow over the surface of a wing, tail plane and wind turbine rotor and so forth. Hence heat transfer and boundary layer flow by a moving surface has wide coverage in the industrial manufacturing procedures. Few examples of such processes may include glass fiber creation, hot moving, paper generation, wire drawing, nonstop throwing, metal turning, metal and polymer expulsion, drawing of plastic movies and so on. The last item in toughening and diminishing of copper wires enormously relies on heat transfer rate at the stretched sheet. Such flow consideration in vicinity of magnetic field has pivotal role in the metallurgical process. Particular motivating flow problems containing non-Newtonian fluid can be found in the studies [1–10].

The investigation of magnetic field has a few restorative and designing applications in improved oil recuperation, magnetohydrodynamics generators, electronic bundles, pumps, thermal insulators, flow meters, power era and so on. The modern

* Corresponding author. Tel.: +92 3009019713.
E-mail address: mikhan@math.qau.edu.pk (M.I. Khan).
Peer review under responsibility of Faculty of Engineering, Alexandria University.

http://dx.doi.org/10.1016/j.aej.2016.04.037
1110-0168 © 2016 Faculty of Engineering, Alexandria University. Production and hosting by Elsevier B.V.

Nomenclature

u, v	velocity components	q_w	surface heat flux
μ	dynamic viscosity	a	radius of cylinder
ρ	fluid density	k_∞	thermal conductivity of ambient fluid
c, β	characteristics of Eyring Powell	K	Hartman number
B_0	magnetic field intensity	τ	extra stress tensor
U_e	free stream velocity	Pr	Prandtl number
U_w	stretching velocity	υ	kinematic viscosity
K^*	variable thermal conductivity	Nu_x	local Nusselt number
T	temperature	Cf_x	skin friction coefficient
T_∞	ambient temperature	Re_x	local Reynolds number
l	characteristics length	ε	small scaler parameter
σ	Electrical conductivity	γ	curvature parameter
a, b	dimensional constant	θ	dimensionless temperature
T_w	uniform temperature over the surface	λ	fluid parameter

devices are bothered by the collaboration between the electrically leading liquid and the magnetic field. The flow act solidly builds upon the orientation and the intensity of the applied magnetic field. The suspended particles are molded by applied magnetic field. In boundary layer flow the force and heat exchange by stretched surface are controlled by MHD. Hayat et al. [11] studied MHD flow of nanofluid over permeable stretching sheet with convective boundary conditions. Raju et al. [12] considered nanofluid by a nonlinear permeable stretched surface with three dimensional (MHD) flow. Hayat et al. [13] studied Cattaneo–Christov heat flux in MHD flow of Oldroyd-B fluid with homogeneous-heterogeneous reactions. Magnetohydrodynamic three-dimensional flow of nanofluid by a porous shrinking surface is studied by Hayat et al. [14]. Sandeep et al. [15] worked on comparative study of convective heat and mass transfer in non-Newtonian nanofluid flow past a permeable stretching sheet. Turkyilmazoglu [16] found the exact solution of MHD flow over three dimensional deforming bodies. Zaidi et al. [17] analyzed MHD effects in two dimensional wall jet flow with convective heat transfer. Unequal diffusivities case of homogeneous-heterogeneous reactions within viscoelastic fluid flow in the presence of induced magnetic field and nonlinear thermal radiation is studied by Annimasun et al. [18]. Rashidi and Erfani [19] considered analytical method for solving steady MHD convective and slip flow due to a rotating Disk with Viscous Dissipation and Ohmic Heating. Heat and mass transfer in MHD non-Newtonian bio-convection flow over a rotating cone/plate with cross diffusion is analyzed by Raju and Sandeep [20]. Mixed convective heat transfer for MHD viscoelastic fluid flow over a porous wedge with thermal radiation is considered by Rashidi et al. [21]. Raju et al. [22] considered dual solutions of MHD boundary layer flow past an exponentially stretching sheet with non-uniform heat source/sink.

The Powell–Eyring model discussed in [23] becomes more composite and deserves our attention because it has certain advantages over the Power-law model and Prandtl–Eyring model. The theory of rate processes is used to derive the Eyring–Powell model for describing the shear of a non-Newtonian flow. In some cases this model predicts the viscous behavior of polymer solutions and viscoelastic suspension over a wide range of shear rates. Eyring–Powell model is used to describe the shear rates of non-Newtonian flow. Impacts of magnetohydrodynamics (MHDs) and thermal radiation in flow of Eyring–Powell liquid are reported by Hayat et al. [24]. Analysis of Eyring–Powell liquid over a stretched surface is presented by Javed et al. [25]. Impact of heat transfer in unsteady stretched flow of Eyring–Powell liquid is presented by Khader and Megahed [26]. Elbade et al. [27] studied the flow of Eyring-Powell liquid saturating porous medium. Recently effects of radiation in flow of Eyring–Powell nanofluid are explored by Hayat et al. [28]. Raju et al. [29] studied heat and mass transfer in MHD Eyring–Powell nanofluid flow due to cone in porous medium.

The present analysis discusses the (MHD) stagnation point flow Powell–Eyring fluid by a stretching cylinder. Numerical solutions by using shooting technique are obtained and compared with the analytical solutions derived by homotopy analysis method (HAM) [30–45]. Also the obtained results through graphs and tabulated values are examined for various emerging parameters. Comparison for numerical and analytic solution is excellent.

2. Formulation

Here magnetohydrodynamic (MHD) stagnation point flow of Powell–Eyring fluid toward a stretching cylinder is considered (see Fig. 1). The fluid is assumed electrically conducting in the presence of a uniform magnetic field. Induced magnetic and

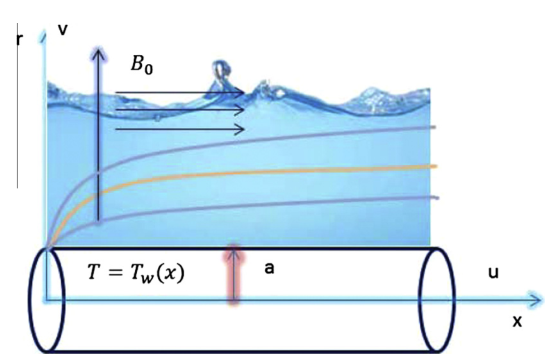

Figure 1 Geometry of the problem.

electric fields are ignored. It is also assumed that thermal conductivity changes linearly with temperature. Heat transfer is also studied. Expression of an extra stress tensor τ in Powell–Eyring fluid is

$$\tau = \mu\nabla V + \frac{1}{\beta}\sinh^{-1}\left(\frac{1}{c}\nabla V\right) \quad (1)$$

$$\sinh^{-1}\left(\frac{1}{c}\frac{\partial u_i}{\partial x_j}\right) \cong \frac{1}{c}\frac{\partial u_i}{\partial xj} - \frac{1}{3!}\left(\frac{1}{c}\frac{\partial u_i}{\partial x_j}\right)^3; \quad \left|\frac{1}{c}\frac{\partial u_i}{\partial x_j}\right|. \quad (2)$$

Here β and c represent the characteristics of Eyring–Powell fluid.

The equations which can discuss the present flow are [28] as follows:

$$\frac{\partial(ru)}{\partial x} + \frac{\partial(rv)}{\partial r} = 0, \quad (3)$$

$$u\frac{\partial u}{\partial x} + v\frac{\partial u}{\partial r} = \left(v + \frac{1}{\beta\rho c}\right)\frac{\partial^2 u}{\partial r^2} - \frac{1}{2\beta c^3\rho}\left(\frac{\partial u}{\partial r}\right)^2\frac{\partial^2 u}{\partial r^2} + \frac{1}{r}\left(v + \frac{1}{\beta\rho c}\right)\frac{\partial u}{\partial r} - \frac{1}{6\beta r\rho c^3}\left(\frac{\partial u}{\partial r}\right)^3 - \frac{\sigma B_0^2}{\rho} \times (u - U_e) + U_e\frac{\partial U_e}{\partial x}, \quad (4)$$

$$u\frac{\partial T}{\partial x} + v\frac{\partial T}{\partial r} = \frac{1}{\rho r c_p}\frac{\partial}{\partial r}\left(k^*(T) r\frac{\partial T}{\partial r}\right). \quad (5)$$

The associated boundary conditions are

$$u(x,a) = U_w(x) = \frac{U_0 x}{l}, \; v = 0, \; T(x,a) = T_w(x) = T_\infty + T_0\left(\frac{x}{l}\right) \text{ at } r = a, \quad u(x,a) \to U_e(x) = \frac{U_\infty x}{l}, \; T(x,a) \to T_\infty \text{ as } r \to \infty. \quad (6)$$

Here u and v represent the velocity components in the x and r directions respectively, v the kinematic viscosity, ρ the density, k the variable thermal conductivity, T the fluid temperature, T_∞ the ambient temperature, U_w the stretching velocity, U_e the free stream velocity, and a and b represent the dimensional constants. The variable thermal conductivity $k^*(T)$ is given by [32]:

$$k^*(T) = k_\infty(1 + \varepsilon\theta) \quad (7)$$

where k_∞ is the thermal conductivity of the ambient liquid, θ the dimensionless temperature and ε a small scalar parameter which demonstrates the impact of temperature on variable thermal conductivity.

Considering [28]:

$$\eta = \sqrt{\frac{u_0}{vl}}\left(\frac{r^2 - a^2}{2a}\right), \quad u = \frac{u_0 x}{l}f'(\eta), \quad \upsilon = -\frac{a}{r}\sqrt{\frac{vU_0}{l}}f(\eta), \quad \theta(\eta) = \frac{T - T_\infty}{T_w - T_\infty}, \quad (8)$$

Eq. (3) is automatically satisfied while Eqs. (4)–(6) take the form of

$$(1 + 2\gamma\eta)(1 + M)f''' + ff'' - (f')^2 + 2\gamma(1 + M)f'' - \frac{4}{3}\lambda M\gamma(1 + 2\gamma\eta)(f'')^3 - M\lambda(1 + 2\gamma\eta)^2(f'')^2 f''' - K^2(f' - A) + A^2 = 0 \quad (9)$$

$$(1 + 2\gamma\eta)\theta'' + 2\gamma\theta' + \varepsilon[(1 + 2\gamma\eta)((\theta')^2 + \theta\theta'') + 2\gamma\theta\theta'] + Prf\theta' = 0 \quad (10)$$

$$f(0) = 0, \quad f'(0) = 1, \quad f'(\infty) = A, \quad \theta(0) = 1, \quad \theta(\infty) = 0. \quad (11)$$

Here γ, A, λ, M, K and Pr denote curvature parameter, ratio parameter, fluid parameter, fluid material parameter, Hartman number and Prandtl number. These are defined through the values:

$$\gamma = \sqrt{\frac{vl}{U_0 a^2}}, \quad A = \frac{U_\infty}{U_0}, \quad \lambda = \frac{U_0^3 x^2}{2l^2 c^2 v}, \quad M = \frac{1}{\mu\beta c}, \quad K = \sqrt{\frac{\sigma\beta_0^2 l}{\rho U_0}}, \quad Pr = \frac{\mu c_p}{k}, \quad (12)$$

Skin friction coefficient and local Nusselt number are

$$C_f = \frac{\tau_w}{\rho U_w^2}, \quad Nu_x = \frac{xq_w}{k(T_w - T_\infty)}, \quad (13)$$

$$\tau_w = \left[\mu\left(\frac{\partial u}{\partial r}\right) + \frac{1}{\beta c}\frac{\partial u}{\partial r} - \frac{1}{6\beta c^3}\left(\frac{\partial u}{\partial r}\right)^3\right]_{r=a}, \quad q_w = -k\left(\frac{\partial T}{\partial r}\right)_{r=a}. \quad (14)$$

In dimensionless variables one has

$$\frac{1}{2}C_f Re_x^{1/2} = (1 + M)f''(0) - \frac{M\lambda}{3}(f''(0))^3, \quad Nu_x Re_x^{-1/2} = -\theta'(0) \quad (15)$$

where $Re_x = U_w l/v$ indicate the local Reynolds number.

3. Comparison between homotopy analysis and shooting solutions

See Fig. 2 and Table 1.

4. Homotopic solutions

The initial guesses and linear operators for momentum and temperature equations are

$$f_0(\eta) = A\eta + (1 - A)(1 - \exp(-\eta)), \quad \theta_0(\eta) = \exp(-\eta), \quad (16)$$

$$\mathcal{L}_f(\eta) = \frac{d^3 f}{d\eta^3} - \frac{df}{d\eta}, \quad \mathcal{L}_\theta(\eta) = \frac{d^2\theta}{d\eta^2} - \theta \quad (17)$$

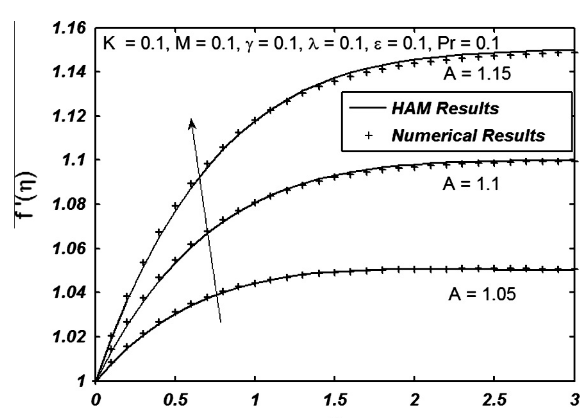

Figure 2 Comparison between HAM and shooting solutions.

Table 1 Comparative studies of HAM and shooting computations of $f'(\eta)$ for Prandtl number Pr and small temperature parameter ε when $\gamma = 0.1$, $A = 0.1$, $\beta = 2$, $K = 0.2$, $\lambda = 0.1$ and $\eta \to 0$.

ε	0.1		0.2		0.3		0.4	
Pr	HAM	Shooting	HAM	Shooting	HAM	Shooting	HAM	Shooting
1.0	−0.5035	−0.5035	−0.4569	−0.4569	−0.3979	−0.3979	−0.3203	−0.3203
1.2	−0.5224	−0.5224	−0.4747	−0.4747	−0.4151	−0.4151	−0.3371	−0.3371
1.3	−0.5731	−0.5731	−0.4838	−0.4838	−0.4238	−0.4238	−0.3456	−0.3456
1.4	−0.5416	−0.5416	−0.4929	−0.4929	−0.4325	−0.4325	−0.3541	−0.3541

with

$$\mathcal{L}_f[A_1 + A_2\exp(\eta) + A_3\exp(-\eta)] = 0, \tag{18}$$

$$\mathcal{L}_\theta[A_4\exp(\eta) + A_5\exp(-\eta)] = 0, \tag{19}$$

where A_i ($i = 1$–5) are arbitrary constants. Through homotopy procedure boundary conditions, and the values for A_i ($i = 1$–5) are

$$A_3 = A_5 = 0, \quad A_2 = \left.\frac{\partial f^\star_m(\eta)}{\partial\eta}\right|_{\eta=0}, \quad A_1 = -A_2 - f^\star_m(0), \\ A_4 = -\theta^*_m(0). \tag{20}$$

4.1. Optimal convergence control parameters

The series solution contains the non-zero auxiliary parameters $\hbar_f$ and $\hbar_\theta$, which determine the convergence region and also rate of the homotopy series solutions. To get the optimal values of $\hbar_f$ and $\hbar_\theta$, we have utilized the concept of minimization by defining the average squared residual errors as proposed by Liao [30]:

$$\varepsilon^f_m = \frac{1}{k_1+1}\sum_{j=0}^{k}\left[N_f\left(\sum_{m=0}^{\infty}f(\eta), \sum_{m=0}^{\infty}g(\eta)\right)_{\eta=j\delta\eta}\right]^2 d\eta \tag{21}$$

$$\varepsilon^g_m = \frac{1}{k_1+1}\sum_{j=0}^{k}\left[N_g\left(\sum_{m=0}^{\infty}f(\eta), \sum_{m=0}^{\infty}g(\eta)\right)_{\eta=j\delta\eta}\right]^2 d\eta. \tag{22}$$

Following Liao [30] we have

$$\varepsilon^t_m = \varepsilon^f_m + \varepsilon^g_m \tag{23}$$

where ε^t_m is the total squared residual error, $\delta\eta = 0.5$ and $k_1 = 21$. Total average squared residual error is minimized by using Mathematica package BVPh2.0 which can be found at http://numericaltank.sjtu.edu.cn/BVPh2.0. The basic concept is to minimize the total average squared residuals and finding out the corresponding local optimal convergence control parameters. For example, a case has been considered where $\gamma = 0.1$, $K = 0.1$, $A = 0.1$, $\varepsilon = 0.1$, $\lambda = M = 0.2$ and Pr 1.5. The optimal values of convergence control parameters at 4th order of approximations are $\hbar_f = -1.4608$ and $\hbar_\theta = -1.20705$.

4.2. Convergence of HAM solutions

HAM provides us great freedom to select initial guesses for momentum and temperature equations. Now the solutions of equations (9) and (10) with the boundary condition (11) are computed using HAM. We have plotted the $\hbar$-curves for $f''(0)$ and $\theta'(0)$ in Fig. 3. From Fig. 3, we can see that the admissible ranges of $\hbar_f$ and $\hbar_\theta$ are $-1.9 \leqslant \hbar_f \leqslant -0.3$ and $-1.8 \leqslant \hbar_\theta \leqslant -0.4$.

Table 2 shows the convergence of functions $f''(0)$ and $\theta'(0)$ at different order of approximations. Tabulated values show that 14th order of approximation is enough for the convergence of $f''(0)$ and 18th order of approximation is appropriate for the convergence of $\theta'(0)$ (see Tables 3 and 4).

4.3. Discussion

In this subsection we will disclose the variations of physical parameters on the velocity and temperature.

4.4. Dimensionless velocity distribution

Velocity distribution for various values of Hartman number (K) on f' is sketched in Fig. 4. Velocity and boundary layer thickness decrease with an increase in Hartman number. Because Lorentz force increases for higher values of K, which is a resistive force. As a result velocity of the fluid decreases. Fig. 5 depicts the influence of fluid material parameter M on velocity distribution. Velocity profile enhances for larger values of M. Because the elasticity of the material increases due to which velocity of the fluid particle enhances. Fig. 6 shows the behavior of ratio parameter A on velocity distribution. Higher values of A result in enhancement of velocity distribution. It is noted that velocity boundary layer thickness has opposite behavior for $A > 1$ and $A < 1$. For $A < 1$ the velocity of the fluid particles is less than the stretching velocity of

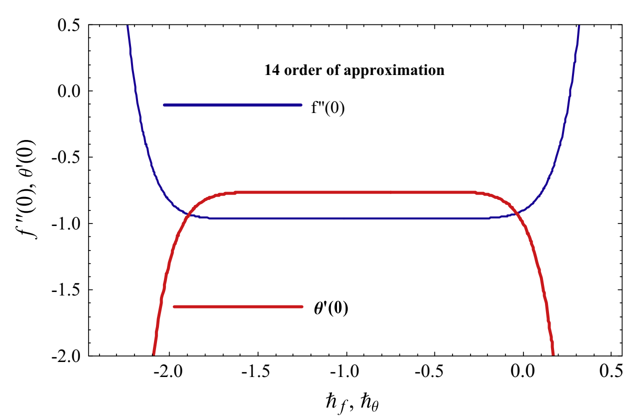

Figure 3 $\hbar$-curves for f and θ.

Table 2 Convergence of series solutions via $\gamma = 0.1$, $K = 0.1$, $A = 0.1$, $\varepsilon = 0.1$, $\lambda = M = 0.2$ and $Pr = 1.5$.

Order of approximations	$-f''(0)$	$-\theta'(0)$
1	0.9391	0.8740
5	0.9658	0.7646
8	0.9662	0.7614
10	0.9662	0.7617
12	0.9662	0.7619
14	0.9662	0.7620
16	0.9662	0.7620
18	0.9662	0.7620

Table 3 The variation of $C_f Re_x^{1/2}$ with respect to K, M, λ, γ and A.

K	M	λ	γ	A	$2(1+M)f''(0) - \frac{2M\lambda}{3}(f''(0))^3$
0.1	0.1	0.1	0.1	0.1	−2.1197
0.3					−2.2733
0.4					−2.3478
0.2	0.2				−2.3007
	0.3				−2.4007
	0.4				−2.4977
0.3	0.3	0.2			−2.4846
		0.3			−2.4793
		0.4			−2.4740
0.1		0.3	0.1	0.4	−1.8141
			0.2		−1.8299
			0.3		−1.8558
	0.4			0.1	−2.4669
				0.2	−2.3264
				0.3	−2.1451

Table 4 Local Nusselt number $-\theta'(0) = Nu_x Re_x^{-1/2}$ via ε, Pr and K.

K	ε	Pr	$-\theta'(0)$
0.2	0.1	1.5	0.79292
0.3			0.82343
0.4			0.85378
0.2	0.2		0.74581
	0.3		0.70529
	0.4		0.67000
	0.1	1.3	0.73068
		1.4	0.76233
		1.5	0.79292

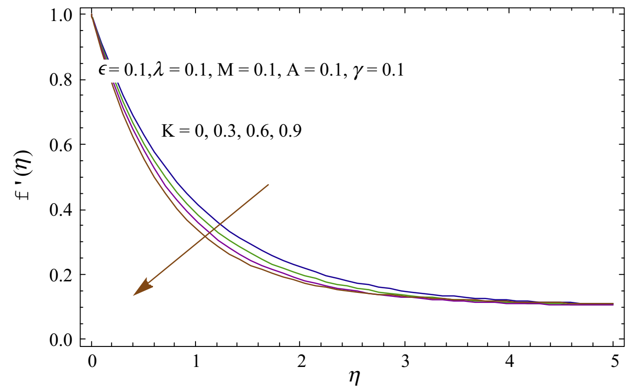

Figure 4 Impact of K on f'.

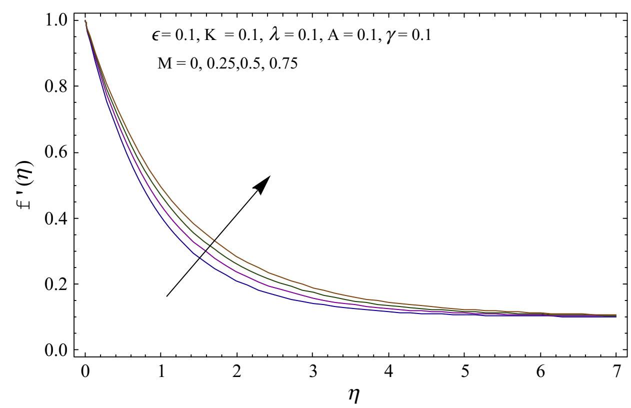

Figure 5 Impact of M on f'.

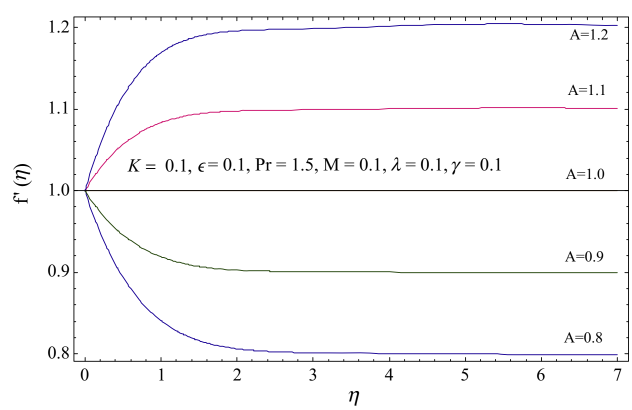

Figure 6 Impact of A on f'.

the cylinder. For $A = 1$ there exists no boundary layer due to the fact that fluid and cylinder move with the same velocity.

4.5. Dimensionless temperature distribution

Impact of curvature parameter on temperature profile is sketched in Fig. 7. The drawn results show increasing behavior of temperature profile for higher values of γ. For higher value of γ, the radius of cylinder diminishes which infers that area of the cylinder with fluid declines. Thus heat transfer is extra frequent over surface of cylinder. This happens because of temperature enhancement. Further boundary layer is thickened for larger values of γ. Fig. 8 analyzes the performance of ε on temperature profile. It is noticed that temperature of the fluid enhances via increase in thermal conductivity ε. An increase in kinetic energy of the fluid particle enhances the heat transfer. Fig. 9 shows the behavior of Prandtl number Pr on temperature profile. For increasing value of Prandtl number the temperature decreases. Higher values of Pr correspond to low thermal diffusivity and the fluid temperature decreases. It can be seen that temperature distribution decreases via increase in Prandtl number Pr. Larger Prandtl number leads to a decrease in thermal diffusivity.

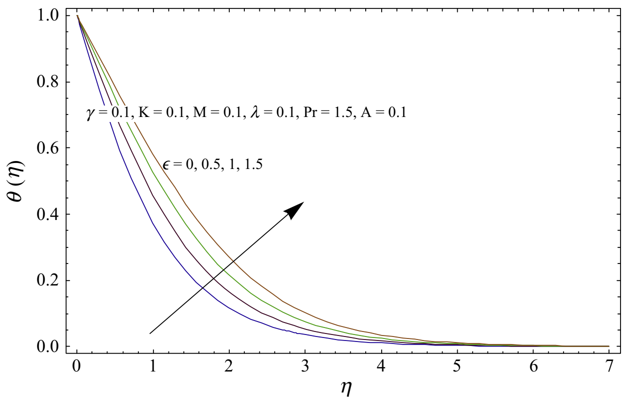

Figure 7 Impact of ε on θ.

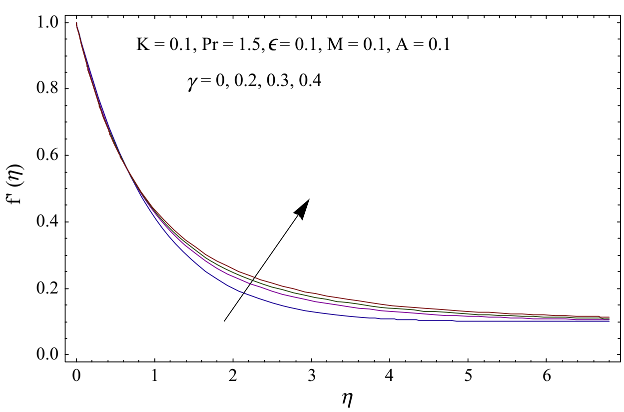

Figure 8 Impact of γ on θ.

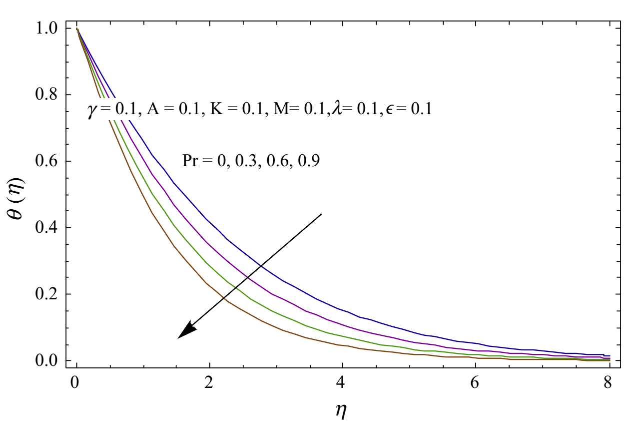

Figure 9 Impact of Pr on θ.

4.6. Concluding remarks

This paper examined the effects of Hartman number and variable thermal conductivity in the flow Powell–Eyring fluid by a stretching cylinder. Such motivation is due to scarce literature on stretching cylinder subject to non-Newtonian fluid of variable physical properties. Major points of the presented analysis are given below.

- Both velocity and temperature profiles enhance for increasing the values of curvature parameter.
- Velocity distribution has decreasing behavior for higher values of Hartman number.
- Effects of Powell–Eyring fluid parameters on velocity profile are quite opposite.
- Velocity profile increases while the temperature profile decreases as fluid parameter M increases.
- Temperature profile enhances for increasing the value of thermal conductivity.
- Behaviors of fluid material parameters M and λ are quite opposite.
- Temperature profile decreases for increasing the Prandtl number Pr.
- Temperature and velocity show qualitative behavior when $A \lesseqgtr 1$.

References

[1] O.D. Makinde, On thermal stability of a reactive third grade fluid in a channel with convective cooling the walls, Appl. Math. Comput. 213 (2009) 170–176.

[2] T. Hayat, A. Shafiq, A. Alsaedi, MHD axisymmetric flow of third grade fluid by a stretching cylinder, Alex. Eng. J. 54 (2015) 205–212.

[3] T. Hayat, S. Qayyum, M. Imtiaz, A. Alsaedi, Impact of Cattaneo–Christov heat flux in Jeffrey fluid flow with homogeneous–heterogeneous reactions, PLoS ONE 11 (2016) e0148662.

[4] R. Ellahi, A study on the convergence of series solution of non-Newtonian third grade fluid with variable viscosity, Adv. Math. Phys. 2012 (2012) 634925.

[5] T. Hayat, M. Waqas, S.A. Shehzad, A. Alsaedi, Stretched flow of Carreau nanofluid with convective boundary condition, Pram. J. Phys. 86 (2016) 3–17.

[6] T. Hayat, M. Waqas, S.A. Shehzad, A. Alsaedi, MHD stagnation point flow of Jeffrey fluid by a radially stretching surface with viscous dissipation and Joule heating, J. Hydrol. Hydromech. 63 (2016) 311–317.

[7] T. Hayat, S. Farooq, B. Ahmad, A. Alsaedi, Characteristics of convective heat transfer in the MHD peristalsis of Carreau fluid with Joule heating, AIP Adv. 6 (2016) 045302.

[8] T. Hayat, S. Qayyum, M. Imtiaz, A. Alsaedi, Three-dimensional rotating flow of Jeffrey fluid for Cattaneo–Christov heat flux model, AIP Adv. 6 (2016) 025012.

[9] M.M. Rashidi, N.V. Ganesh, A.K.A. Hakeem, B. Ganga, Buoyancy effect on MHD flow of nanofluid over a stretching sheet in the presence of thermal radiation, J. Mol. Liquids 198 (2014) 234–238.

[10] T. Hayat, M. Imtiaz, A. Alsaedi, MHD 3D flow of nanofluid in presence of convective conditions, J. Mol. Liquids 212 (2015) 203–208.

[11] T. Hayat, M. Imtiaz, A. Alsaedi, MHD flow of nanofluid over permeable stretching sheet with convective boundary conditions, Ther. Sci. (2014), http://dx.doi.org/10.2298/TSC1140819139H.

[12] C.S.K. Raju, N. Sandeep, M.J. Babu, V. Sugunamma, Dual solutions for three-dimensional MHD flow of a nanofluid over a nonlinearly permeable stretching sheet, Alex. Eng. J. 55 (2016) 151–162.

[13] T. Hayat, M. Imtiaz, A. Alsaedi, S. Almezal, On Cattaneo–Christov heat flux in MHD flow of Oldroyd-B fluid with homogeneous-heterogeneous reactions, J. Magn. Magn. Mater. 401 (2016) 296–303.

[14] T. Hayat, M. Imtiaz, A. Alsaedi, M.S. Alhuthali, Magnetohydrodynamic three-dimensional flow of nanofluid by

a porous shrinking surface, J. Aerosp. Eng. (2015) 04015035, http://dx.doi.org/10.1061/(ASCE)AS.1943-5525.0000533.
[15] N. Sandeep, B.R. Kumar, M.S.J. Kumar, A comparative study of convective heat and mass transfer in non-Newtonian nanofluid flow past a permeable stretching sheet, J. Mol. Liquids 212 (2015) 585–591.
[16] M. Turkyilmazoglu, An analytical treatment for the exact solutions of MHD flow and heat over two–three dimensional deforming bodies, Int. J. Heat Mass Transf. 90 (2015) 781–789.
[17] S. Zulfiqar, A. Zaidi, S.T. Mohyud-Din, Convective heat transfer and MHD effects on two dimensional wall jet flow of a nanofluid with passive control model, Aero. Sci. Technol. 49 (2016) 225–230.
[18] I.L. Annimasun, C.S.K. Raju, N. Sandeep, Unequal diffusivities case of homogeneous–heterogeneous reactions within viscoelastic fluid flow in the presence of induced magnetic field and nonlinear thermal radiation, Alex. Eng. J. 55 (2) (2016) 1595–1606.
[19] M.M. Rashidi, E. Erfani, Analytical method for solving steady MHD convective and slip flow due to a rotating disk with viscous dissipation and ohmic heating, Eng. Comput. 29 (2012) 562–579.
[20] C.S.K. Raju, N. Sandeep, Heat and mass transfer in MHD non-Newtonian bio-convection flow over a rotating cone/plate with cross diffusion, J. Mol. Liquids 215 (2016) 115–126.
[21] M.M. Rashidi, M. Ali, N. Freidoonimehr, B. Rostami, M.A. Hossain, Mixed convective heat transfer for MHD viscoelastic fluid flow over a porous wedge with thermal radiation, Adv. Mech. Eng. 2014 (2014) 735939.
[22] C.S.K. Raju, N. Sandeep, C. Sulochana, M.J. Babu, Dual solutions of MHD boundary layer flow past an exponentially stretching sheet with non-uniform heat source/sink, J. Appl. Fluid Mech. 9 (2016) 555–563.
[23] R.E. Powell, H. Eyring, Mechanisms for the relaxation theory of viscosity, Nature 154 (1944) 427–428.
[24] T. Hayat, M. Awais, S. Asghar, Radiative effects in three-dimensional flow of MHD Eyring–Powell fluid, J. Egypt. Math. Soc. 21 (2013) 379–384.
[25] T. Javed, N. Ali, Z. Abbas, M. Sajid, Flow of an Eyring–Powell non-Newtonian fluid over a stretching sheet, Chem. Eng. Commun. 200 (2013) 327–336.
[26] M.M. Khader, A.M. Megahed, Numerical studies for flow and heat transfer of the Powell–Eyring fluid thin film over an unsteady stretching sheet with internal heat generation using the Chebyshev finite difference method, J. Appl. Mech. Tech. Phys. 54 (2013) 444–450.
[27] N.T.M. Eldabe, S.N. Sallam, M.Y. Abou-Zeid, Numerical study of viscous dissipation effect on free convection heat and mass transfer of MHD non-Newtonian fluid flow through a porous medium, J. Egypt. Math. Soc. 20 (2012) 139–151.
[28] T. Hayat, N. Gull, M. Farooq, B. Ahmad, Thermal radiation effect in MHD flow of Powell–Eyring nanofluid induced by a stretching cylinder, J. Aerosp. Eng. 29 (2015) 04015011.
[29] M.J. Babu, N. Sandeep, C.S.K. Raju, Heat and Mass transfer in MHD Eyring–Powell nanofluid flow due to cone in porous medium, Int. J. Eng. Resear. Afr. 19 (2016) 57–74.
[30] S.J. Liao, An optimal homotopy-analysis approach for strongly nonlinear differential equations Commun, Nonlinear Sci. Numer. Simulat. 15 (2010) 2003–2016.
[31] T. Hayat, M. Waqas, S.A. Shehzad, A. Alsaedi, A model of solar radiation and Joule heating in magnetohydrodynamic (MHD) convective flow of thixotropic nanofluid, J. Mol. Liquids 215 (2016) 704–710.
[32] T. Hayat, M. Waqas, S.A. Shehzad, A. Alsaedi, Mixed convection flow of viscoelastic nanofluid by a cylinder with variable thermal conductivity and heat source/sink, Int. J. Numer. Methods Heat Fluid Flow 26 (2016) 214–234.
[33] S. Abbasbandy, M. Yurusoy, H. Gulluce, Analytical solutions of non-linear equations of power-law fluids of second grade over an infinite porous plate, Math. Comput. Appl. 19 (2014) 124–133.
[34] T. Hayat, M. Farooq, A. Alsaedi, Homogeneous–heterogeneous reactions in the stagnation point flow of carbon nanotubes with Newtonian heating, AIP Adv. 5 (2015) 027130.
[35] Y. Lin, L. Zheng, X. Zhang, L. Ma, G. Chen, MHD pseudo-plastic nanofluid unsteady flow and heat transfer in a finite thin film over stretching surface with internal heat generation, Int. J. Heat Mass Transf. 84 (2015) 903–911.
[36] T. Hayat, M. Farooq, A. Alsaedi, F. Al-Solamy, Impact of Cattaneo–Christov heat flux in the flow over a stretching sheet with variable thickness, AIP Adv. 5 (2015) 087159.
[37] A. Malvandi, F. Hedayati, M.R.H. Nobari, An HAM analysis of stagnation point flow of a nanofluid over a porous stretching sheet with heat generation, J. Appl. Fluid Mech. 7 (2014) 135–145.
[38] T. Hayat, M.I. Khan, M. Farooq, A. Alsaedi, M. Waqas, T. Yasmeen, Impact of Cattaneo–Christov heat flux model in flow of variable thermal conductivity fluid over a variable thicked surface, Int. J. Heat Mass Transf. 99 (2016) 702–710.
[39] T. Hayat, M.I. Khan, M. Farooq, T. Yasmeen, A. Alsaedi, Stagnation point flow with Cattaneo–Christov heat flux and homogeneous-heterogeneous reactions, J. Mol. Liquids 220 (2016) 49–55.
[40] T. Hayat, Zakir Hussain, A. Alsaedi, B. Ahmad, Heterogeneous-homogeneous reactions and melting heat transfer effects in flow with carbon nanotubes, J. Mol. Liquids 220 (2016) 200–207.
[41] M. Khan, W.A. Khan, Forced convection analysis for generalized Burgers nanofluid flow over a stretching sheet, AIP Adv. 5 (2015) 107138.
[42] M. Khan, W.A. Khan, Steady flow of Burgers nanofluid over a stretching surface with heat generation/absorption, J. Braz. Soc. Mech. Sci. Eng. (2015), http://dx.doi.org/10.1007/s40430-014-0290-4.
[43] M. Turkyilmazoglu, Solution of Thomas–Fermi equation with a convergent approach, Commun. Nonlinear Sci. Numer. Simulat. 17 (2012) 4097–4103.
[44] T. Hayat, M. Rashid, M. Imtiaz, A. Alsaedi, Magnetohydrodynamic (MHD) stretched flow of nanofluid with power-law velocity and chemical reaction, AIP Adv. 5 (2015) 117121.
[45] T. Hayat, M. Imtiaz, A. Alsaedi, Effects of homogeneous–heterogeneous reactions in flow of Powell–Eyring fluid, J. Cent. South Univ. 22 (2015) 3211–3216.